High-resolution Acoustic Camera on CR200 and Post-Processing

*Jin-Yeong Park, Hyuk Baek, Pan-Mook Lee and Bong-Huan Jun
Ocean System Engineering Research Division, Maritime Ocean Engineering Research Institute
Korea Institute of Ocean Science & Technology (KIOST)
*jinyeong96@gmail.com

***Abstract*- This paper describes applications of high-resolution acoustic camera for a multi-legged underwater robot, CR200. CR200 has six legs and is supposed to inspect and work in high tidal current and low visibility environment. Performance of optical cameras are limited and their viewing range becomes less than a couple of meters. A multi-beam acoustic camera can be a substitute for the optical cameras for inspecting and surveying as an identification sensor. In this paper, we introduce an acoustic camera, ARIS, which uses 3.0MHz, the highest frequency. The ARIS shows 2.9mm downrange resolution with 5m range in identification mode. Comparison of the ARIS and a multi-beam sonar using 900kHz is present briefly. And then, we introduces post-processing for 3-dimensional object model reconstruction using multiple acoustic 2-dimensional images. Results of underwater experiments of CR200 and ARIS are also included.**

I. Introduction

A bio-inspired underwater walking robot, CR200 has been developed in KIOST (Korea Institute of Ocean Science & Technology). [1] The most interesting feature of the robot is to use six legs to thrust itself and to control its attitude. It controls its body attitude increasing downward lift force against tidal current. In addition, it can move on the seabed without disturbing sediment or something else in the floor. This robot is supposed to inspect and survey in high current and turbid seabed. Figure 1 shows the CR200 preparing launch at a pier.

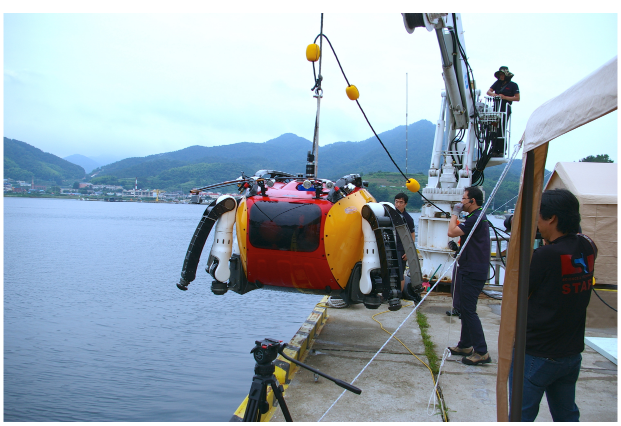

Figure 1. Launch of CR200 at the pier in SSRI
(South Sea Research Institute, KIOST)

In the area with high tidal current, there are thick turbidity and lots of floating matters. Therefore conventional optical cameras are able to show only strongly limited performance. An acoustic camera using multi-beam can be a substitute for the optical camera system. Its validity as an alternative to the optical systems has been verified through various previous researches. The acoustic camera can be a candidate for an obstacle avoidance, gap-filler aiding side-scan sonar and identification sensor for underwater vehicles [2] Ref. [3] and [4] introduce real-time object recognition using high resolution acoustic camera which is installed on an AUV (Autonomous Underwater Vehicle). Acoustic camera DIDSON (Dual Frequency Identification Sonar) was adopted to image objects. DIDSON can operate at two frequency modes, 1.8MHz and 1.0MHz. Automatic detection of underwater chain links using a forward looking sonar was described in [5]. They uses ARIS (Adaptive Resolution Imaging Sonar) from Sound Metrics [6]. The ARIS also operates at two frequency modes in the same manner with DIDSON but higher frequencies, i.e 3.0MHz and 1.8MHz, are used with maximum downrange resolution, 2.9mm.

We adopted ARIS sonar as an identification sensor for CR200. As the CR200 is able to keep its position and body attitude stationary from external disturbances such as current, we expect ARIS to image in more detail.

In section 2, we introduce CR200, a new type of ROV (Remotely Operated Vehicle) briefly. And the acoustic camera, ARIS will be described. Its role as an identification sensor for CR200 and benefits are presented. In section 3, the experiments and images will be explained. Image comparison with a multi-beam sonar using 900kHz is also included. The authors could take some acoustic images in the pier during the first diving test of CR200. Post-processing to construct-3-dimensional object modeling are in section 4. Conclusions and summary are in section 5.

II. CR200 & ARIS

A. CR200

CR200 has six legs; frontal two legs of them are manipulator -combined legs with total 7 degree of freedoms and the others are dedicated legs having 4 degree of freedoms. Overall design and configuration of CR200 are present in [1]. Two pressure housing vessels contains electric systems. Two junction boxes are installed on both side of the robot to distribute signals and power. Figure 2 shows appearance of CR200. Specifications of CR200 is denoted in Table 1. Mechanical design, implementation and control of manipulators and legs were investigated by [7] and [8]. Finite element analysis of the body frame for CR200 was also conducted. [9] The body frame of CR200 was made of carbon fiber reinforced plastic (CFRP) to be lighter and stronger than any frame of the other conventional materials. Ref. [10] describes operating software for CR200. The CR200 system is similar to conventional ROV system having remote control unit.

B. ARIS Explorer 3000

Full model name of ARIS we adopted is "ARIS Explorer 3000." 3.0MHz is the highest frequency among worldwide products of acoustic cameras. As a result, ARIS shows the most precise downrange resolution at the high frequency mode (Identification mode). But, valid range is relatively short, 5m. Table 2 shows specifications of the ARIS. For convenience, 2-axis rotator is also widely used. X2 rotator from Sound Metrics is adopted. Roll and tilt motion bounds are 0^{o} ~ -90^{o} and 30^{o} ~ -90^{o}, respectively. ARIS and X2 are shown in Fig. 3.

C. Integration

Installation of ARIS on CR200 is shown in Fig. 4. Figure 5 describes block diagrams of wiring and connection of the ARIS. As there is no actuator or rotator for panning motion, CR200 have to rotate its whole body to pan the ARIS. Acoustic beams forming a wedge shaped volume are projected from the ARIS. (Fig. 6) The minimum start range is 0.7m and the maximum end range is dependent on which mode is adopted. The end ranges of identification mode and detect mode are 5m and 15m, respectively.

TABLE I. SPECIFICATIONS OF CR200

Items	Value	Unit	Remarks
Dimension	2.5 × 2 × 1.3(1.8)	m	sit (stand)
Weight	646kg @ air 154kg @ water	kgf	
Depth	200	m	
Power	20	kW	
Walking speed	0.5	m/s	
Equipment	Acoustic camera, Scanning sonar, ADCP, CTD, AHRS, USBL, Altimeter, Tool sled, Pan/Tilt optical HD camera, Contact force sensors		

Figure 2. CR200 is standing on six legs

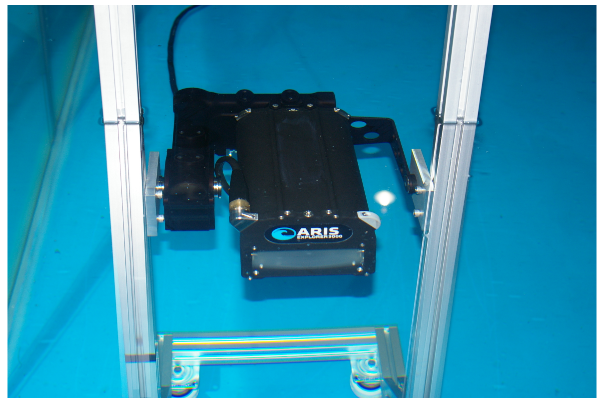

Figure 3. ARIS Explorer 3000 and X2 rotator

Figure 4. ARIS and X2 rotator installed on CR200

TABLE II. SPECIFICATIONS OF ARIS

	Operating Frequency	Beamwidth	Number of Beams	Range
Identification mode	3.0MHz	0.25	128	5m
Detection mode	1.8MHz	0.42	128 or 64	15m
Frame rate	**Field of view**	**Power consumption**	**Weight @ air**	**Dimension**
30 fps (max.)	30^{o} H, 14^{o} V	15W	5kg	26×16×14 cm

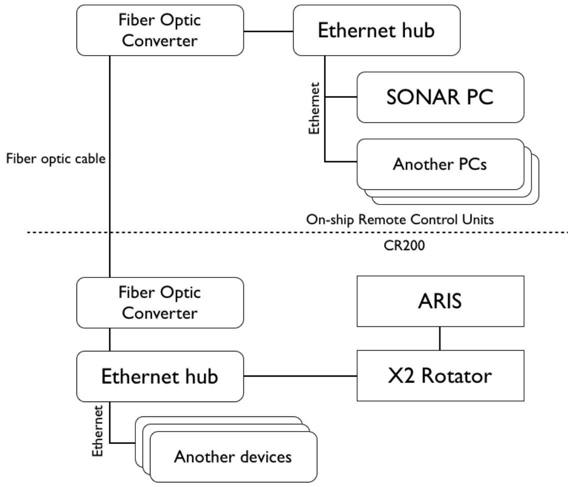

Figure 5. Block diagram

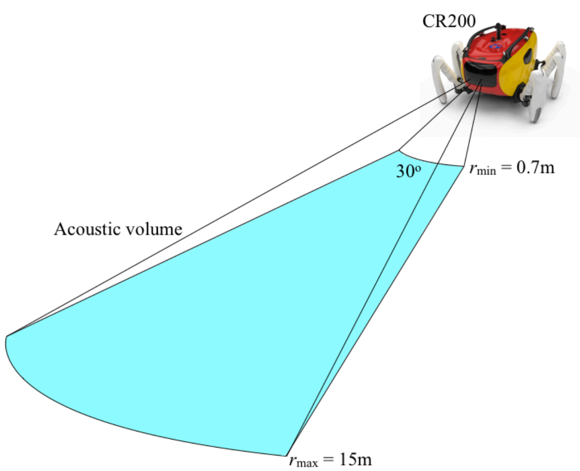

Figure 6. Acoustic volume projected by the ARIS from CR200
(Areas extended by roll and tilt motions are not depicted.)

s

Figure 7. Target subject

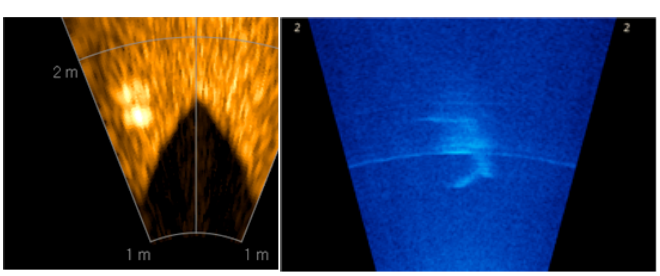

Figure 8. (Left) Image from P900-45, (Right) Image from ARIS

III. Underwater Images

A.-Image comparison

We conducted underwater experiments to compare ARIS images with another multi-beam sonar. P900-45 from BlueView [11] was used. It operates at 900kHz. A target subject is shown in Fig. 7. The target has a circular plate with 25cm diameters and three pod legs. As we can expected, ARIS's images showed higher resolution displaying the target and its pod legs. From images of P900-45, we could detect the target as a brighter spot. The three pod legs could not be identified, however. (Fig. 8)

B. CR200's diving test at the pier

CR200's first diving test was accomplished at the pier in SSRI. Figure 9 and 10 show images from the optical HD camera and the ARIS, respectively. Some kinds of fish were detected. They were swimming in front of the robot. As CR200 doesn't use any propellers, fish could come much closer to the robot and were not frightened. In addition, the CR200 was able to move its position on the floor and to turn its sight direction without disturbing sediment as we expected. Several starfish were also inspected by the ARIS. They moved very slowly. Ripraps were also detected.

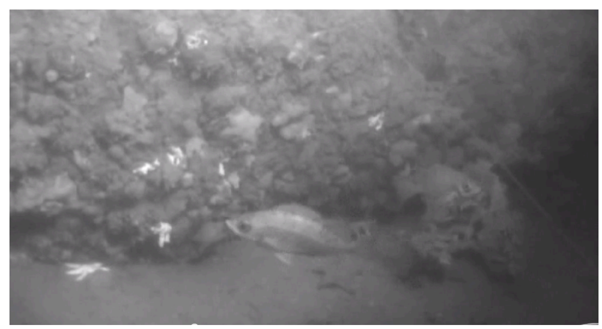

Figure 9. Image from the optical HD camera

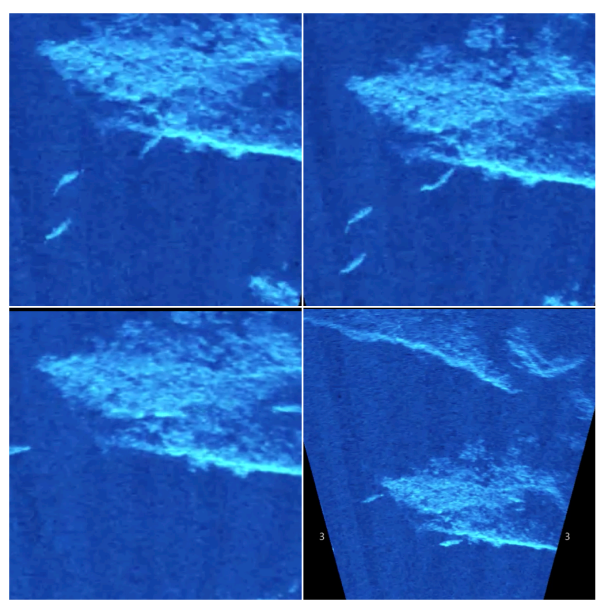

Figure 10. Images from the ARIS - Fish and ripraps

IV. Post-processing

We achieved preliminary study on post processing to extract 3D whole body model of the target projected on multiple acoustic 2D images. This was inspired by CT (Computerized Tomography.) Basically, the acoustic camera supplies 2D images composed of two set of data; intensity and distance. Ref. [12] defines the sonar coordinate system as shown in Fig. 11. The symbol of r is range between the ARIS and point ***P***, where θ is the azimuth and φ is the elevation of the point. The acoustic camera does not provide elevation φ. Therefore for a given point ***P*** in the image, it can lie anywhere on a vertical arc at a fixed range, spanning the vertical beam width. [12] In the case of the ARIS, vertical beam width is 14°. We assumed all points in the single image lies on the same plane where elevation φ is zero. For example, ***P*** was assumed to be projected at ***P'***. Experiments were conducted in the water basin as shown in Fig. 12. For simplicity, we grabbed acoustic images with tilting motion only. The processing consists of several stages as follows.

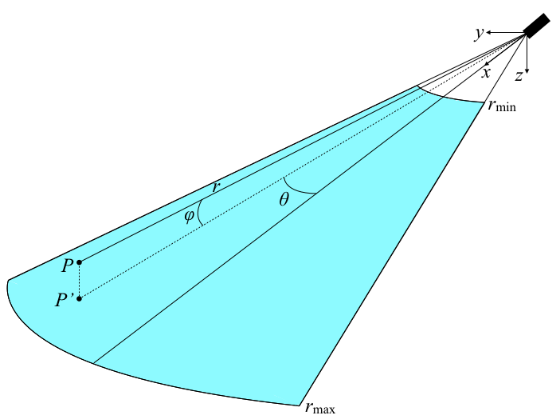

Figure 11. Coordinate system for the ARIS

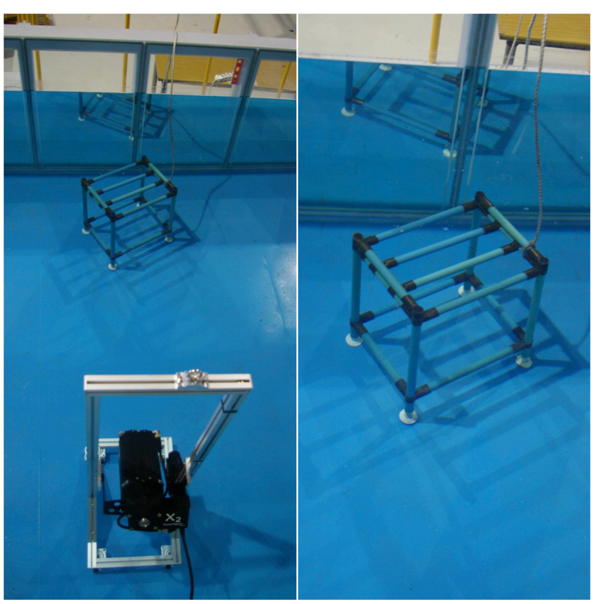

Figure 12. (Left) ARIS and target in the basin. (Right) The target

Stage (1)*: Target imaging with tilt motion*

We operated ARIS to image the target in order and grabbed acoustic images consecutively as shown in Fig. 13 and 14. Y and Z axes are parts of the global coordinate. The symbol of Φ_k is tilt angle of the acoustic camera when the k^{th} image is grabbed. It can be measured by the sensor built in the camera.

Stage (2)*: Select the points with higher intensity*

To discriminate the target from background, points whose intensity is higher than pre-specific threshold, I_{th} were selected. The threshold value was determined by trial-and-error. Let $I(\cdot)$ be the intensity function of the corresponding point. Points which satisfy the following equation (1) were collected. Superscript k means that the point ***P'*** is in the k^{th} image and subscript S means that ***P'*** is expressed with respect to the sonar coordinate in Fig. 11. Result is shown in Fig. 15. This process was repeated n times for all n images.

$$I\left(P'\big|_S^k\right) \geq I_{th} \qquad (1)$$

Stage (3)*: Coordinate conversion*

Coordinate with respect to the sonar coordinate and the global coordinate are denoted by subscripts S and G, respectively. As the horizontal viewing angle range of the ARIS are bounded between -15° and 15°, azimuth θ with respect to the sonar coordinate and azimuth Θ with respect to the global coordinate are very close. In addition, range R with respect to the global coordinate can be approximated to r. Elevation of the k^{th} image with respect to the global coordinate is Φ_k. As we ignored elevation in the single image, ***P*** became ***P'*** and as a result, point ***P'*** can be denoted as the following equations (2). Then, we can express ***P'*** on the k^{th} image with respect to the global and spherical coordinate system as the following equation (3).

Discussion

Result is shown in Fig. 16. The exact 3D model could not be reproduced. Vertical pillars and horizontal beams are discriminated roughly. Because there is finite vertical beam width, we can not recognize the exact elevation of points in the wedge shaped acoustic energy volume. As a result, distortions could not be avoided, especially, in the case of some parts where elevation changes dramatically in the single acoustic volume.

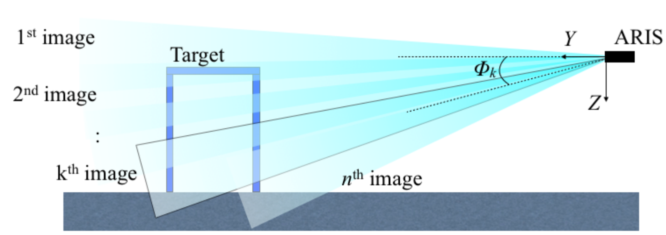

Figure 13. Target imaging with tilting (Sideview)

$$P|_S = \begin{bmatrix} x \\ y \\ z \end{bmatrix}_S = \begin{bmatrix} r\cos\phi\cos\theta \\ r\cos\phi\sin\theta \\ r\sin\phi \end{bmatrix}_S \quad (2)$$

$$P'|_S = \begin{bmatrix} x \\ y \end{bmatrix}_S = \begin{bmatrix} r\cos\theta \\ r\sin\theta \end{bmatrix}_S$$

$$P'|_G^k = \begin{bmatrix} R \\ \Theta \\ \Phi_k \end{bmatrix}_G^k \quad (3)$$

where, $R \approx r$ and $\Theta \approx \theta$.

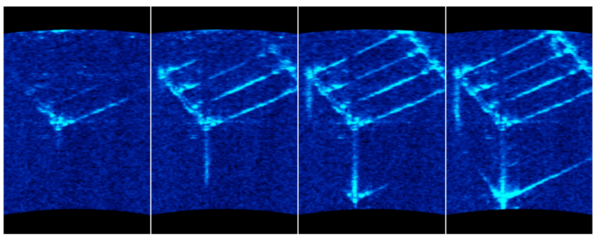

Figure 14. Acoustic images grabbed consecutively

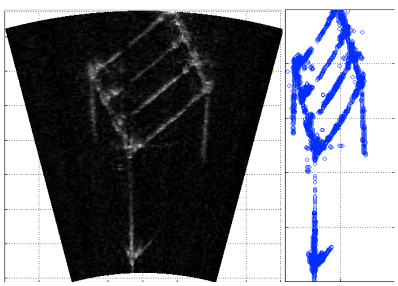

Figure 15. (Left) Raw image, (Right) Processed image

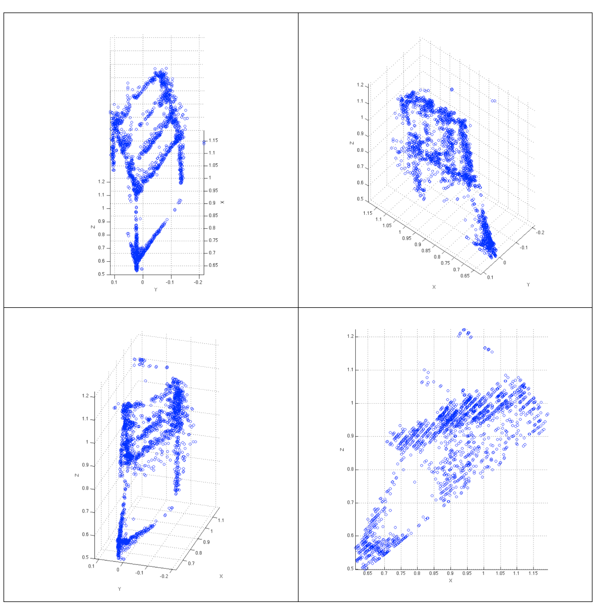

Figure 16. Results of 3D modeling.

V. CONCLUSIONS

In this paper, we introduced underwater walking robot, CR200 and ARIS acoustic camera. The ARIS was integrated in CR200 system successfully and showed its feasibility as an identification sensor through the underwater tests. Post processing to re-construct 3D model of the subjects was proposed. Using multiple 2D acoustic images and attitude data of the acoustic camera, we tried to extract spatial shape of the target. The proposed method could not imitate the original target shape exactly, however, because of lack of elevation information and effect of finite vertical beam width. In spite of distortions, the re-constructed model helps us to guess the entire shape of subjects.

ACKNOWLEDGMENT

This work was supported by the Ministry of Oceans and Fisheries (MOF) of Republic of Korea for "*Development of multi-legged walking and flying subsea robot*."

REFERENCES

[1] Jun, B. H., Shim, H., Kim, B., Park, J. Y., Baek, H., Yoo, S. and Lee, P. M., "Development of Seabed Walking Robot CR200," *OCEANS'13 MTS/IEEE Bergen*, 2013.

[2] Belcher, E.O., Fox, W.L.J. and Hanot, W.H., "Dual Frequency Acoustic Camera: A Candidate for an Obstacle Avoidance, Gap-Filler and Identification Sensor for Untethered Underwater Vehicle," *Proceedings of OCEANS'02 MTS/IEEE,* pp.2124-2128, 2002.

[3] Yu. S.C., Kim, T.W., Asada, A., Weatherwax, S., Collins, B., and Yuh, J., "Development of High-Resolution Acoustic Camera based Real-Time Object Recognition System by using Autonomous Underwater Vehicles," *Proceedings of OCEANS'06 MTS/IEEE Boston*, 2006.

[4] Yu. S.C., "Development of real-time acoustic image recognition system using by autonomous marine vehicle," *Ocean Engineering*, Vol. 35, Issue 1., pp.90-105, 2008.

[5] Hurtós, N., Palomeras, N., Nagappa, S. and Salvi, J., "Automatic Detection of Underwater Chain Links using a Forward Looking Sonar," *Proceedings of OCEANS'13 MTS/IEEE Bergen*, 2013

[6] Sound Metrics Corp. [Online] www.soundmetrics.com

[7] Kang, H., Shim, H., Jun, B.H. and Lee, P.M., "Development of Leg with Arm for the Multi-Legged Seabed Robot "CR200"," *Proceedings of OCEANS'12 MTS/IEEE Hampton road*, 2012

[8] Shim, H., Jun, B.H., Kang, H., Yoo, S., Lee, G.M. and Lee, P.M., "Development of Underwater Robotic Arm and Leg for Seabed Robot, CRABSTER200," *Proceedings of OCEANS'13 MTS/IEEE Bergen*, 2013

[9] Yoo. S., Jun, B.H., Shim, H., Lee, P.M., and Kim, B., "Finite Element Analysis of Carbon Fiber Reinforced Plastic Body Frame for Seabed Robot, Crabster200," *Proceedings of OCEANS'13 MTS/IEEE Bergen*, 2013.

[10] Kim, B., Shim, H., Yoo, S., Jun, B.H, Park, S.W. and Lee, P.M., "Operating Software for a Multi-legged Subsea Robot CR200," *Proceedings of OCEANS'13 MTS/IEEE Bergen*, 2013.

[11] BlueView Technologies, Inc. [Online] www.blueview.com

[12] Seto, Mae L., "Marine Robot Autonomy," *Springer*, 2013